Redox Biology 67 (2023) 102903

Contents lists available at ScienceDirect

Redox Biology

journal homepage: www.elsevier.com/locate/redox

ADAR1 exacerbates ischemic brain injury via astrocyte-mediated neuron apoptosis

Dunpeng Cai [a], Mikayla Fraunfelder [a], Ken Fujise [b], Shi-You Chen [a,c,*]

[a] Departments of Surgery, University of Missouri School of Medicine, Columbia, MO, USA
[b] Harborview Medical Center, Department of Medicine, University of Washington, Seattle, WA, USA
[c] The Research Service, Harry S. Truman Memorial Veterans Hospital, Columbia, MO, USA

ARTICLE INFO

Keywords:
ADAR1
Cerebral artery occlusion
Astrocytes
Proliferation
Apoptosis
ROS

ABSTRACT

Astrocytes affect stroke outcomes by acquiring functionally dominant phenotypes. Understanding molecular mechanisms dictating astrocyte functional status after brain ischemia/reperfusion may reveal new therapeutic strategies. Adenosine deaminase acting on RNA (ADAR1), an RNA editing enzyme, is not normally expressed in astrocytes, but highly induced in astrocytes in ischemic stroke lesions. The expression of ADAR1 steeply increased from day 1 to day 7 after middle cerebral artery occlusion (MCAO) for 1 h followed by reperfusion. ADAR1 deficiency markedly ameliorated the volume of the cerebral infarction and neurological deficits as shown by the rotarod and cylinder tests, which was due to the reduction of the numbers of activated astrocytes and microglia. Surprisingly, ADAR1 was mainly expressed in astrocytes while only marginally in microglia. In primary cultured astrocytes, ADAR1 promoted astrocyte proliferation via phosphatidylinositol 3-kinase (PI3K)/Akt pathway. Furthermore, ADAR1 deficiency inhibited brain cell apoptosis in mice with MCAO as well as in activated astrocyte-conditioned medium-induced neurons in vitro. It appeared that ADAR1 induces neuron apoptosis by secretion of IL-1β, IL-6 and TNF-α from astrocytes through the production of reactive oxygen species. These results indicated that ADAR1 is a novel regulator promoting the proliferation of the activated astrocytes following ischemic stroke, which produce various inflammatory cytokines, leading to neuron apoptosis and worsened ischemic stroke outcome.

1. Introduction

Stroke is a leading cause of death and disability worldwide, with ischemic stroke accounting for approximately 87% of all stroke cases in the United States. Ischemic stroke is caused by the occlusion of carotid or cerebral arteries, leading to impaired brain perfusion [1,2]. Although thrombolytic therapy corrects this arterial occlusion if delivered within the first 3–4.5 h of onset, reactive oxygen species (ROS), depolarization, and acute inflammatory responses in the infarct core and the surrounding ischemic penumbra still cause long-term cognitive and psychomotor deficits [3–5]. Moreover, many patients do not even receive effective treatment due to the short time window for intervention or contraindications, making the research on treatment strategies for ischemic stroke a global priority.

In the ischemic penumbra, poor perfusion leads to activation of neural microglia and astrocytes, promoting the production of inflammatory cytokines, increased permeability of the blood-brain barrier (BBB), and migration of leukocytes across the BBB, exacerbating neuron death via necrosis, autophagy, and apoptosis in the initial period following stroke [3–5]. Astrocytes are the most abundant type of glial cells in the mammalian central nervous system (CNS), outnumbering neurons, and their contact and interaction with parenchymal cells enable them to have a significant impact on brain function. However, the roles of astrocytes in ischemic stroke are complex, as they play dual roles in both emergency and repair processes. Some astrocyte-derived factors have multiple or diametrically opposite properties, highlighting the complex nature of astrocyte involvements in stroke pathology. Additionally, even though the formation of a glial scar can isolate the injured area from healthy tissue, a later glial scar can worsen inflammation, inhibit axon growth, and hinder the recovery of motor function. The complex roles of astrocytes in stroke highlight the need for further understanding of the underlying mechanisms involved in acute ischemic brain inflammation.

Therapies targeting inflammatory cascades have been an active area of study in the past two decades. However, increasing evidence suggest

* Corresponding author. Department of Surgery, University of Missouri School of Medicine, 1 Hospital Drive, Columbia, MO, 65212, USA.
E-mail address: scqvd@missouri.edu (S.-Y. Chen).

https://doi.org/10.1016/j.redox.2023.102903
Received 4 September 2023; Received in revised form 19 September 2023; Accepted 22 September 2023
Available online 29 September 2023

Abbreviation

ADAR1	Adenosine deaminase acting on RNA1
BBB	Blood-brain barrier
CNS	Central nervous system
GFAP	Glial fibrillary acidic protein
MCAO	Middle cerebral artery occlusion
OGD	Oxygen-Glucose-Deprivation
ERK	Extracellular signal-regulated kinase
Akt	Ak strain transforming/protein kinase B
WT	Wild type
IL-1β	Interleukin-1β
IL-6	Interleukin-6
TNF-α:	Tumor necrosis factor alpha
ROS	reactive oxygen species

that widespread immunosuppression and inflammation inhibition is deleterious to the long-term stroke recovery [6–8]. Therefore, many studies now target the short-term activation and actions of astrocytes and microglia. IL-1β receptor antagonist (IL-1Bra) treatment in conjunction with thrombolysis is currently the only therapy of this kind with clinical promise, and thus there is a strong need for a better understanding of the mechanisms involved in acute ischemic brain inflammation [4,6–8].

Oxidative stress, characterized by an imbalance between the production and removal of reactive oxygen species (ROS), is a pivotal factor in the pathogenesis of ischemic stroke. During ischemia, the overproduction of ROS can cause cellular damage, leading to neuronal death and exacerbation of inflammation [9,10]. The impact of ROS on ischemic stroke extends to the activation of glial cells, disruption of the blood-brain barrier, and modulation of signaling pathways that influence cell survival and apoptosis.

In the search for targeting the short-term activation and actions of astrocytes and microglia, adenosine deaminase acting on RNA (ADAR1)

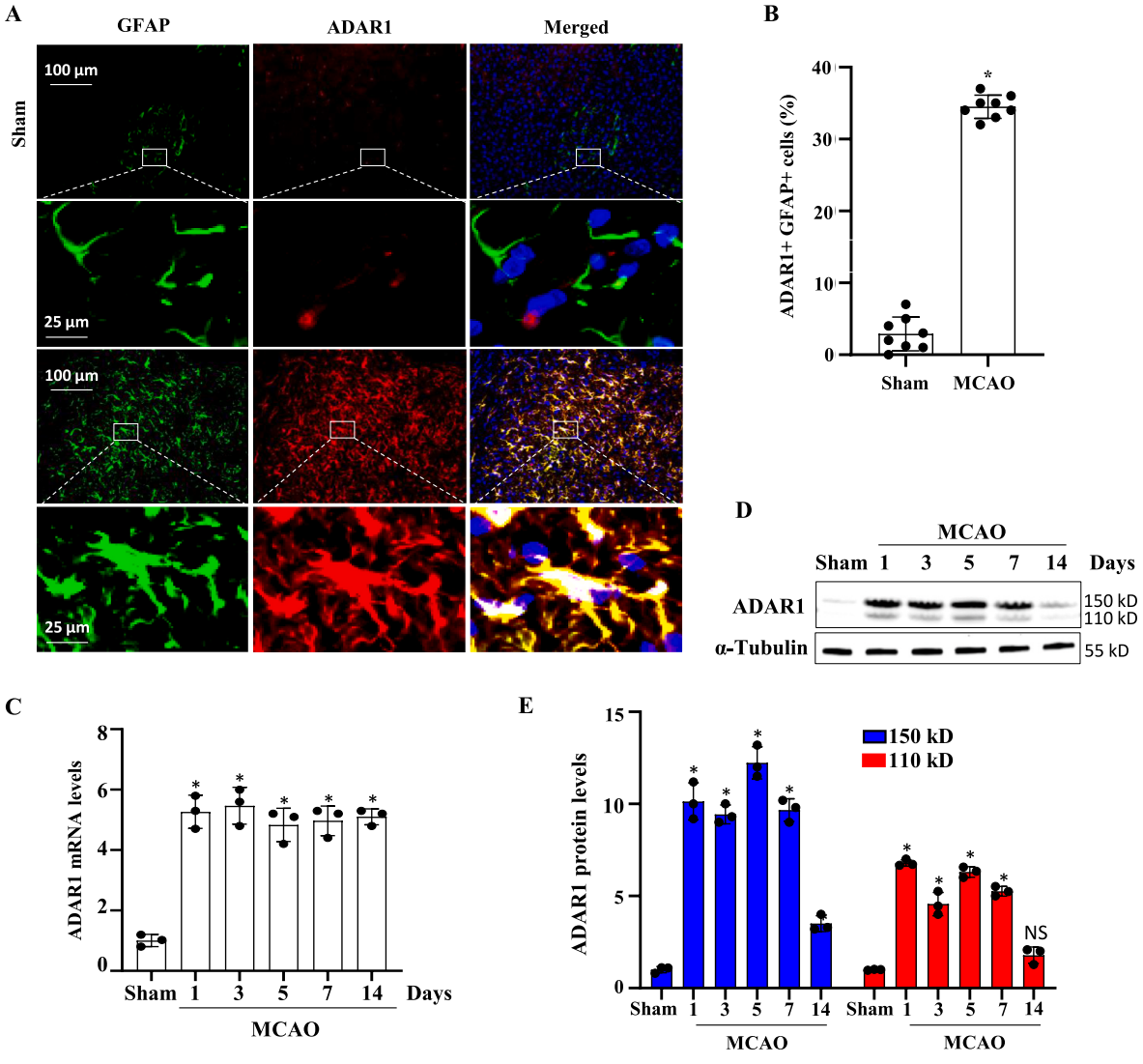

Fig. 1. ADAR1 is induced in astrocytes in ischemic mouse brains with intraluminal middle cerebral artery occlusion (MCAO). Mice were sham-operated or underwent MCAO for 60 min. 7 days later, mice were sacrificed, and ischemic penumbra areas were collected and frozen sectioned. **(A)** ADAR1 expression in glial scar and ischemic area was detected by co-immunostaining with GFAP. **(B)** Quantification of ADAR1+GFAP + cells relative to the total cell numbers in the brain sections. Data are shown as mean ± SD. *P < 0.05 vs Sham group, n = 8. **(C–D)** Mice were sham-operated or underwent MCAO for 60 min. The mice were then euthanized 1, 3, 5, 7, or 14 days later. The ischemic penumbra areas were collected, and RNAs and proteins were extracted followed by RT-qPCR and Western blot analyses to detect ADAR1 mRNA (**C**) and protein expression (**D-E**), respectively. ADAR1 protein levels were quantified by normalizing to α-Tubulin. *P < 0.05, n = 3 in each group. Both p150 and p110 isoforms were significantly induced by MCAO.

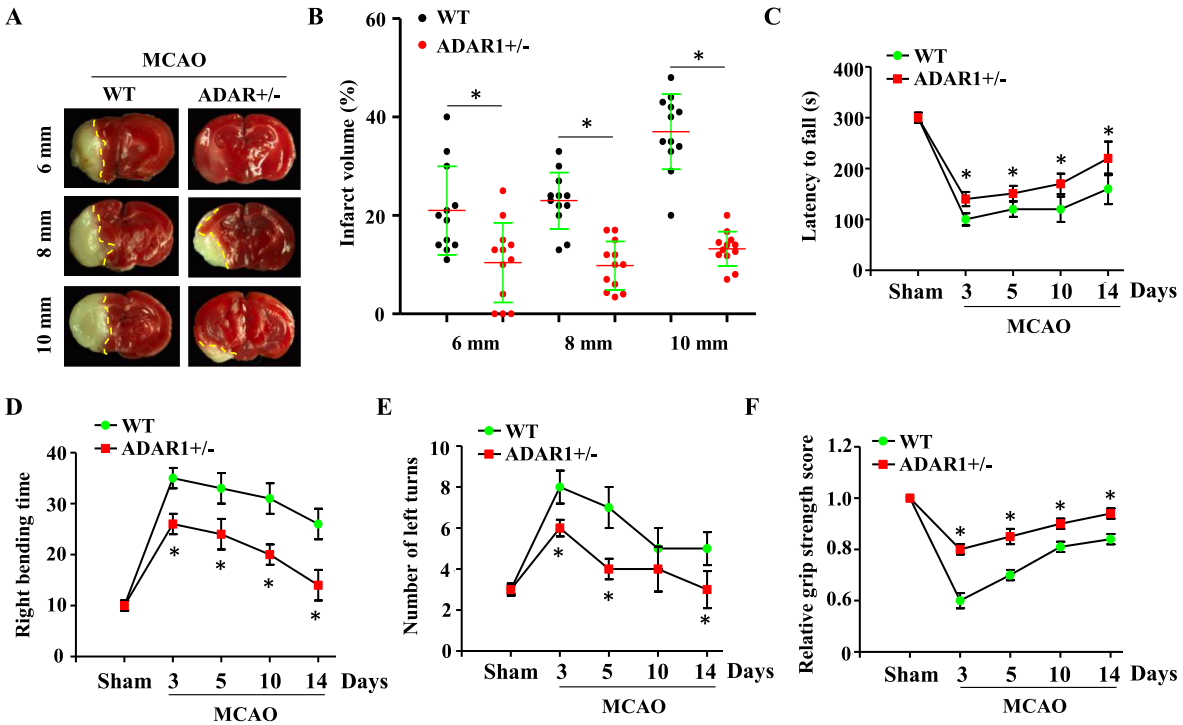

Fig. 2. ADAR1 deficiency decreases brain infarct volumes and improves neurobehavioral outcomes. (A) Mice were sham-operated or underwent MCAO for 60 min. 7 days later, mice were euthanized. Brain sections from WT and ADAR1 ± mice with MCAO were stained with Triphenyltetrazolium chloride (TTC). Shown are sections of anterior (top, 6 mm), middle (8 mm), and posterior (bottom, 10 mm) mouse brain tissues. Red-stained areas indicate normal healthy tissues, whereas the white areas indicate infarcted areas. **(B)** The brain infarction volumes at different distances (6 mm, 8 mm, or 10 mm) from the frontal pole were quantified as percentages of infarcted areas relative to the total brain areas. *P < 0.05, n = 12. ADAR1 ± decreased brain infarct volumes compared to WT mice. **(C–F)** Neurobehavioral tests were conducted 3, 5, 10, or 14 days after the MCAO for both WT and ADAR1 ± mice. The latency to fall in rotarod **(C)**, time spent for right-biased bending in the elevated body swing **(D)**, and grip strength **(E)** were all significantly improved in ADAR1 ± mice compared to WT mice. In addition, WT mice exhibited worse functional impairment in the sensorimotor asymmetry than ADAR1 ± mice in the corner test **(F)**. Plots represent mean ± SD values. *P < 0.05 vs WT group, n = 9. ADAR1 ± attenuated neurobehavioral outcomes after stroke.

shows great potentials. ADAR1 is an RNA-binding protein involved in post-transcriptional RNA editing [11,12] and is over-expressed in lymphocytes in mouse models of microvascular lung injury, sepsis, and acute systemic inflammation, but suppressed in mouse models of pathological liver inflammation [13–15]. Since ADAR1 is significantly induced in astrocytes of mouse brain with ischemic stroke, we postulated that the post-ischemic ADAR1 expression may play a role in the activation of neural glia and the regulation of short-term brain inflammation in stroke brain. To test this hypothesis, we used the middle cerebral artery occlusion (MCAO) rodent stroke model and demonstrated that ADAR1 is indeed responsible for the post-ischemic glial activation and pro-inflammatory cytokine production. Moreover, we found that ADAR1 promotes astrocyte-mediated neuron apoptosis through an inflammatory response due to increased production of reactive oxidative stress (ROS).

2. Materials and methods

2.1. Cytokines and reagents

2,3,5-triphenyl-tetrazolium chloride solution (TTC) and crystal violet (C0775) were purchased from Millipore Sigma (St. Louis, MO). The following antibodies were used in Western blotting and immunofluorescent staining: ADAR1 (D-8, for western blotting), PCNA (PC10), phospho-ERK (sc-7383) and ERK (sc-271269) antibodies were obtained from Santa Cruz Biotechnology. IL-1β (12703), IL-6 (D5W4V), TNF-α (D2D4), cleaved caspase 3 (D3E9), cleaved PARP (D64E10), GFAP (80788), Iba1/AIF-1 (E4O4W), phospho-Akt (D9E) and Akt (9272) antibodies were from Cell Signaling Technology. α-Tubulin (T5168) and Ki-67 antibody were purchased from Sigma. Glyceraldehyde 3-phosphate dehydrogenase (GAPDH) (60004-1-Ig) and ADAR1 (14330-1-AP, for immunofluorescent staining) antibodies were from Proteintech. Nuclei were stained with 4, 6- diamidino-2-phenylindole (DAPI, Vector Laboratories, Inc.). IRDye® 680RD goat anti-rabbit and goat anti-Mouse secondary antibodies were from LI-COR Biosciences. TGF-β (240-B-002) was obtained from R&D Systems. LY294002 (9901) and LY294002 (9901) were obtained from Cell Signaling Technology.

2.2. Animals

ADAR1 heterozygous knockout mice (ADAR+/−, B6.129(Cg)-Adartm1.1Phs/KnkMmjax), were purchased from the Jackson Laboratory (Bar Harbor, ME). All wild type (WT) and ADAR ±mice are in C57BL6 genetic background. Animals were housed under conventional conditions in animal care facilities and received humane care in compliance with the Principles of Laboratory Animal Care formulated by the National Society for Medical Research and the Guide for the Care and Use of Laboratory Animals. All animal procedures were approved by the Institutional Animal Care and Use Committee of the University of Missouri. Animals were randomly grouped, and all operators were blinded to the grouping. Male mice were used in this study in order to determine the potential role of ADAR1 first. The sex difference may be studied in the future. The number of animals (sample size) was determined by power calculation based on the prior experience.

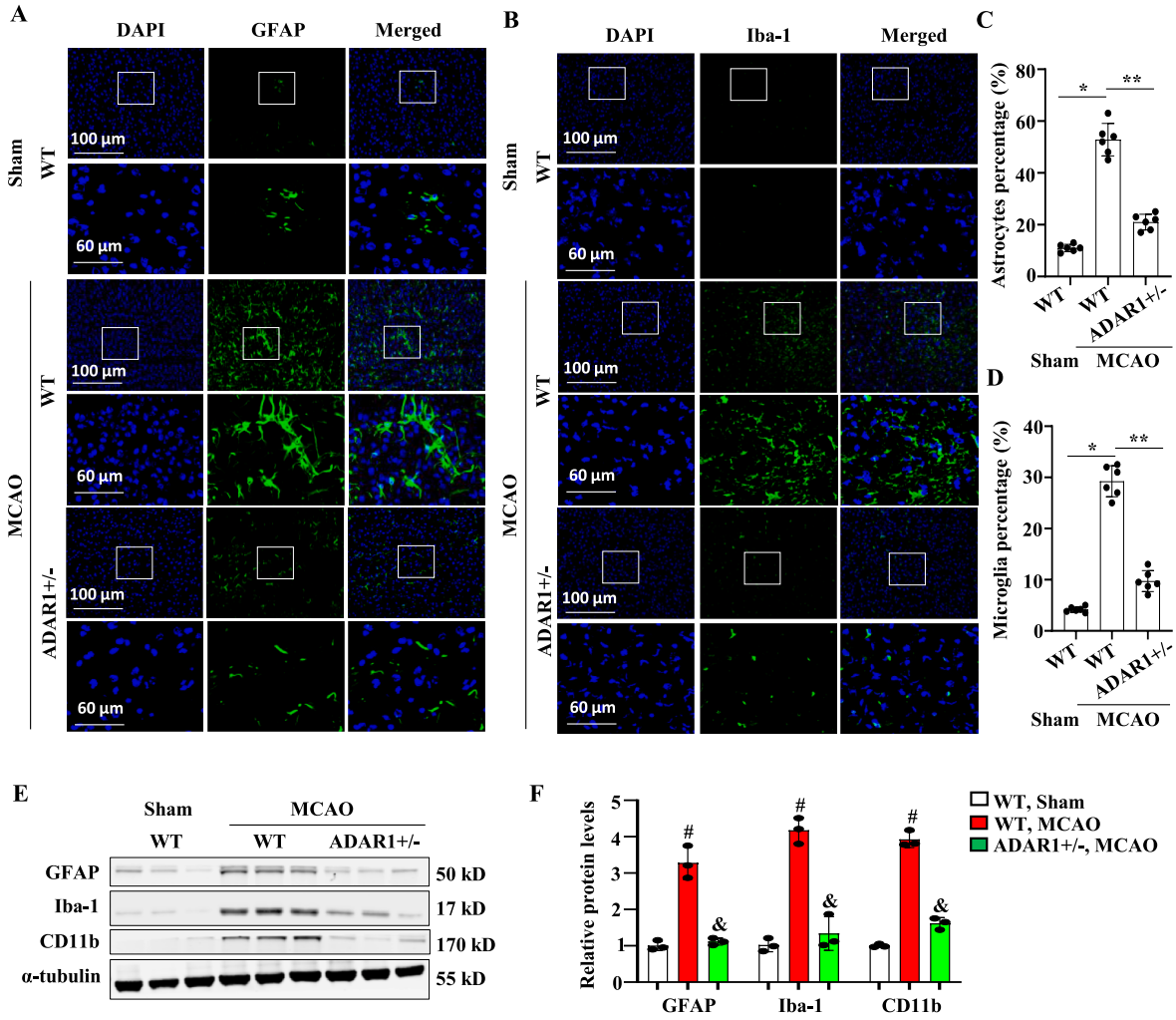

Fig. 3. ADAR1 deficiency inhibits glial cell activation in mouse brain with intraluminal middle cerebral artery occlusion (MCAO). Wild type (WT) or ADAR1 ± **m**ice were sham-operated or underwent MCAO for 60 min. 7 days later, mice were euthanized. **(A)** Immunostaining of astrocytes with glial fibrillary acidic protein (GFAP) in the ischemic areas of mouse brains. **(B)** Immunostaining of microglia/macrophage with specific calcium-binding protein (Iba-1) in the ischemic areas of mouse brains. The higher magnification images for the areas in the rectangles are shown below the images with the rectangles in A-B. **(C-D)** The GFAP + astrocytes (C) and Iba-1+ microglia cells (D) were quantified as % of total cells. *P < 0.01 vs WT group with Sham; **P < 0.01 group vs WT with MCAO; n = 6. **(E)** Western blot analyses of GFAP, Iba-1, and CD11b expressions in ischemic brain of mice. (**F**) Protein levels in E were quantified by normalizing to α-tubulin. #P < 0.01 vs WT group with Sham; &P < 0.01 vs WT group with MCAO; n = 3.

2.3. Middle cerebral artery occlusion (MCAO) and infarct volume measurement

MCAO was generated by the method that produces injury most similar to human stroke, as previously described [16,17]. Briefly, WT C57BL/6J or ADAR1 ± male mice were anesthetized with 5% isoflurane in O2 with a facemask, and the left middle cerebral artery was ligated with 6-0 monofilament nylon (602112PK10, Doccol, Corp., Redlands, CA, United States). After 1 h of occlusion, the monofilament nylon was removed, and reperfusion was initiated. The mice were placed on a homeothermic heating pad to stabilize their body temperature at 37 ± 0.5 °C. Mice in the sham group underwent the same procedure without artery ligation. 1, 3, 5,7 or 14 days later, mice were deeply anesthetized and euthanized with an overdose of isoflurane. Brain tissues were cut into 2-mm coronal sections and then embedded in 2% 2,3,5-triphenyltetrazolium chloride (TTC) (17779, Sigma-Aldrich, United States) or 4% paraformaldehyde (PFA). Two other portions were flash frozen in LN2 and stored in −80C freezer for protein and RNA extraction. The infarct volume was detected and analyzed by using ImageJ v1.37 (NIH, Bethesda, MA, United States) as described previously [53] and presented as a percentage of the volume in the nonischemic hemisphere to correct for edema.

2.4. Grip strength

The grip strength task is a test of neuromuscular performance [18]. Each mouse was held in front of the grip strength device (Lab made) until it grasped the bar. Traction was applied to the mouse's tail until the animal released its grip of the bar. The peak force (in newtons) shown in the Force meter was calculated through Hooke's law, based on the length of the spring. Three trials were performed on each animal and averaged. Post-MCAO grip strength was calculated as a percentage of pre-MCAO grip strength.

2.5. Corner test

A mouse was placed halfway to the corner between two boards each with dimension of 30 × 20 × 1 cm^3 at a 30° angle, arranged with a small opening along the joint between the boards to encourage exploration into the corner [19]. When entering deep into the corner, both sides of the vibrissae approached the wall. The mouse soon reared forward and upward, then turned back to face the open end. The nonischemic mouse

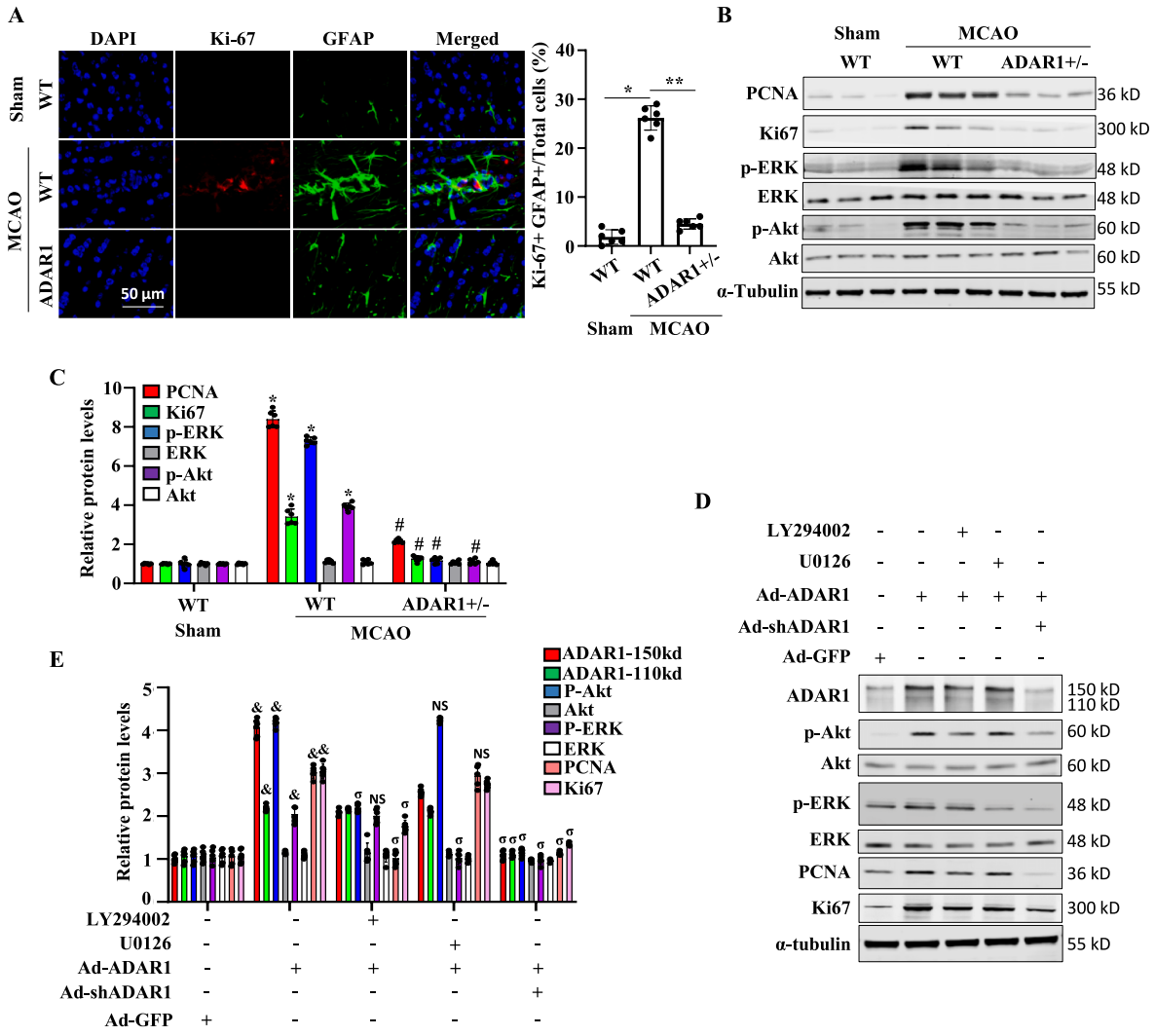

Fig. 4. ADAR1 deficiency inhibits post-stroke proliferation of astrocytes. (A–C) Wild type (WT) or ADAR1 ± **m**ice were sham-operated or underwent MCAO for 60 min. 7 days later, mice were euthanized, and brain tissues collected. **(A)** Astrocyte proliferation in glial scar tissues was detected by co-immunostaining of Ki-67 with GFAP. **(B)** Western blot analyses of PCNA, Ki-67, phospho-ERK, ERK, phospho-Akt, Akt expression in the ischemic brains. **(C)** The protein expression levels in A were quantified by normalizing to α-Tubulin. *P < 0.01 vs. WT group with sham, #P < 0.01 vs. WT group with MCAO; n = 6. **(D, E)** Primary astrocytes were isolated from mouse brain, cultured, transduced with control (Ad-GFP), ADAR1 cDNA (Ad-ADAR1), or ADAR1 shRNA (Ad-shRNA)-expressing adenovirus, and then treated with vehicle (−), PI3/Akt (LY294002), or MEK1/MEK2 (U0126) inhibitor. ADAR1, phospho-Akt (p-Akt), Akt, phospho-ERK (p-ERK), ERK, PCNA, Ki67 expression was detected by Western blot (D) and quantified by normalizing to α-tubulin and relative to the level with Ad-GFP treatment for each protein. &P < 0.05 vs. Ad-GFP group; σP<0.05 vs. Ad-ADAR1 alone group; NS: non-significant; n = 6.

turned left or right with equal frequency, but mouse with unilateral ischemic injury preferentially turned toward the nonimpaired, ipsilateral side (right in our model). The number of turns in each direction was summed from 10 trials. Turning movements that were not a part of a rearing movement were not scored.

2.6. Elevated body swing test (EBST)

The EBST reflects the lateralization of the lesion (asymmetrical motor behavior) [19]. The animal was held approximately 1 cm from the base of its tail [20]. It was then elevated above the surface in the vertical axis. A swing was recorded whenever the animal moved its head out of the vertical axis to either the left or the right side (more than 10°). Before attempting another swing, the animal was momentarily placed back on the ground of his cage. Ten swings were performed for each recording session. The overall number of swings made to the right side was divided by the overall number of swings made to both sides.

2.7. ROS detection by DHE

Dihydroethidium (DHE) was used to detect ROS generation in astrocytes. DHE (D11347, Thermofisher) is a cell-permeating reagent that intercalates within mitochondria DNA, producing a bright red fluorescence when the DNA is oxidized by ROS. Briefly, after being exposed to OGD for 24 h, cells were washed gently with ice cold PBS twice and then incubated with 5 μM of DHE at 37 °C for 20 min in a dark environment. Thereafter the cells were washed with PBS twice to remove free DHE followed by incubation with DAPI for 10 min to visualize nuclei. The cells were then washed with PBS twice and observed under a fluorescent microscope. Bright red fluorescence indicates the production of ROS in the cells. DAPI staining was used to count the total cell number. ROS-producing cell rate was expressed as ROS-positive cell number relative to the total cell number. At least 5 different visual field images per group were used for statistical analyses.

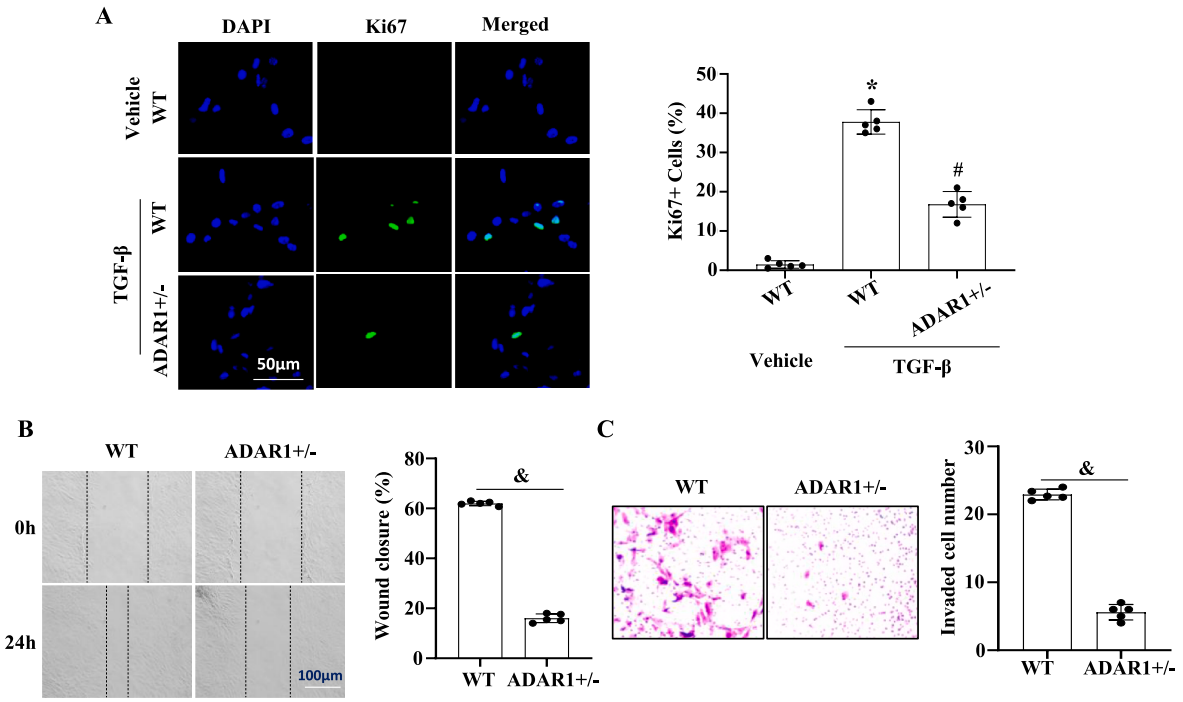

Fig. 5. ADAR1 promotes astrocyte proliferation and migration *in vitro*. Primary cultured astrocytes were isolated from wild type (WT) and ADAR ±mouse brains. (**A**) Ki67 expression in astrocytes treated with vehicle or TGF-β was detected by immunostaining, and Ki67+ cells were quantified relative the total cell numbers. *P < 0.01 vs WT group with vehicle treatment; #p < 0.01 vs WT group with TGF-β treatment, n = 5. **(B)** Confluent monolayers of primary astrocytes from wild type (WT) or ADAR1 ± mice were scratched. The wound healing was observed by an inverted phase-contrast microscope at 0 and 24 h. Shown are representative Images of three independent experiments. Migration rates were calculated as wound closure percentage. &P < 0.01 vs. WT group, n = 5. (**C**) Transwell assay showed that ADAR ±significantly inhibited astrocyte migration. Migrated astrocytes were stained with crystal violet. &P < 0.05 vs. WT group, n = 5.

2.8. Rotarod test

Motor coordination and balance were evaluated with the accelerating-rotarod test as described, with some modifications [21,22]. WT and ADAR1 ± mice were placed on an accelerating rotarod (Fisher, USA) that was programmed to accelerate from 4 to 44 rpm in 3 min and then hold at constant speed for further 2 min. The latency of the mice to fall off the rod was recorded over a maximum observation period of 5 min. Animals were given a session consisting of 3 trials per day with a 20 min inter-trial interval and repeatedly tested for 5 consecutive days. Data from 3 trials were averaged.

2.9. Immunofluorescent staining

Mouse brains were fixed in 4% paraformaldehyde (PFA) and embedded in paraffin. Brain coronal sections (5 μm thick) were processed according to the standard protocol. For immunofluorescent staining, serial sections (5 μm) of OCT-embedded frozen tissues or primary cultured cells were fixed in cold acetone. After blocking with 5% goat serum, sections were incubated with primary antibodies at 4C for 24 h and then with fluorescent dye-conjugated secondary antibodies for 1 h. Images were acquired with a fluorescence microscope (Keyence Corporation of America).

2.10. Western blotting

Brain tissues, astrocytes, or neuron cells were lysed in RIPA lysis buffer (1% Nonidet P-40, 0.1% sodium dodecyl sulfate (SDS), 0.5% sodium deoxycholate, 1 mM sodium orthovanadate, and protease inhibitors) to extract total proteins. Samples were separated on SDS-polyacrylamide gels and electro-transferred onto nitrocellulose membranes or PVDF membrane (Amersham Biosciences). After blocking with 5% BSA, the membranes were incubated with a primary antibody at 4 °C overnight. The membranes were then incubated with IRDye secondary antibodies (LI-COR Biosciences) at room temperature for 1 h. The protein expression was detected and quantified by Odyssey CLx Imaging System (LI-COR Biosciences).

2.11. Terminal deoxy nucleotide transferase-mediated nick-end labeling (TUNEL) assay

The cell apoptosis in brain coronal sections of animals from all groups was analyzed by TUNEL assay using In Situ Cell Death Detection Kit (Roche, Indianapolis, IN) according to the manufacturer's instructions. Briefly, the tissue sections were de-paraffinized, rehydrated, treated with proteinase K working solution, and permeabilized. Permeabilized tissue sections were incubated with the TUNEL reaction mixture in a humidified atmosphere for 60 min at 37 °C in the dark. Sections were counterstained for nuclei with DAPI (Dako, Carpinteria, CA), coverslipped using fluorescent mounting medium (Dako), and observed under a fluorescence microscope (Olympus IX71). The results were quantified by counting the number of TUNEL-positive cells in at least five different ischemic zones of ipsilateral brain region and non-ischemic contralateral brain regions of the tissue sections obtained from at least 8 animals per group.

2.12. Wound healing assay

Astrocytes were replated on polyornithine coated 24 well cell culture plates with Wound healing inserts (Cell Biolabs). The next day, the inserts were then removed to allow the cells to migrate for 24 h. Images of wound healing were captured using a dissection microscope at a magnification of 40x. Cell migration was quantified by blind measuring the migration distances.

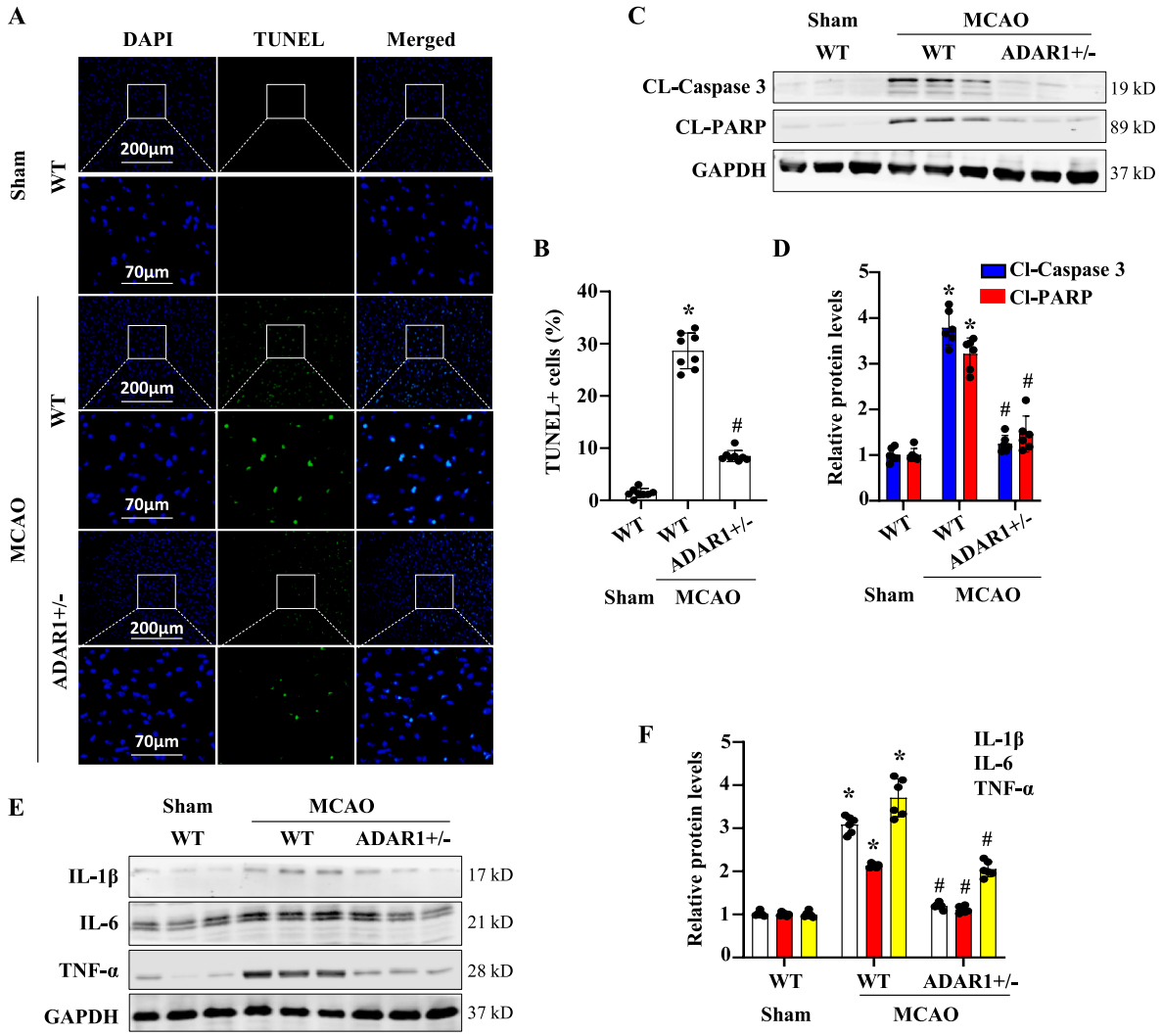

Fig. 6. ADAR1 deficiency inhibits brain cell apoptosis and pre-inflammatory cytokine production in MCAO-operated mice. Wild type (WT) or ADAR1 ± mice were sham-operated or underwent MCAO for 60 min. 7 days later, mice were euthanized, and brain tissues collected. (**A**) TUNEL staining of brain tissue sections. (**B**) TUNEL + cells relative to the total brain cells. *P < 0.01 vs. WT group with Sham; #P < 0.01 vs. WT group with MCAO; n = 8. **(C)** Western blot analyses of cleaved (CL)-Caspase 3 and cleaved (CL)-PARP in ischemic brains. **(D)** Cleaved-Caspase 3 and Cleaved-PARP protein levels were normalized to GAPDH, respectively. *P < 0.01 vs WT group with Sham; #P < 0.01 vs WT group with MCAO; n = 6. **(E)** Western blot analyses of pro-inflammatory cytokines IL-1β, IL-6 and TNF-α in ischemic brains. **(F)** Protein levels shown in E were quantified by normalizing to GAPDH, respectively. *P < 0.01 vs. WT group with Sham; #P < 0.01 vs WT group with MCAO; n = 6.

2.13. Transwell migration assay

Migration of primary cultured astrocytes were measured using 6.5-mm transwell chambers with 8-μm pores (Costar, Cambridge, MA) as described previously [23]. A total of 100 μl of astrocytes cells (1×10^5 cells/ml) was transferred into the top chamber of the transwells and allowed to migrate at 37 °C in 5% CO2. After migration for 48 h, the upper surface of each membrane was cleaned with a cotton swab. Cells attached to the bottom surface of each membrane were stained with 0.1% crystal violet, imaged, and counted using a Nikon inverted microscope. Assays were performed in triplicate for three times.

2.14. Real-time quantitative polymerase chain reaction

Total RNA of brain tissues was extracted using Trizol Reagent (Thermo Scientific, 10296028) and then reverse transcribed to cDNA using iScript cDNA Synthesis kit (Bio-Rad, 1708890) as described previously [24]. Real-time quantitative polymerase chain reaction was performed with Stratagene Mx3005P PCR instrument using SYBR Green master mix (GeneCopoeia, QP001). GAPDH was used as an internal control. Primer sequences are listed as below: ADAR1 Forward: GCC AAA GAC AGT GGT CAA CCA G, ADAR1 Reverse: GAA CAA GGA TGT TGC TGA GGA GC. GAPDH Forward: CAT CAC TGC CAC CCA GAA GAC TG, GAPDH Reverse: ATG CCA GTG AGC TTC CCG TTC AG.

2.15. Astrocyte isolation

Highly enriched primary astrocytes were prepared from the cerebral cortex of 2–3 months old male mice. After mice were euthanized by CO_2 overdose, cerebral cortexes were aseptically dissected, and meninges were carefully removed. Several superficial washings were performed with phosphate buffered saline (PBS) containing 100 U/mL penicillin and 100 μg/mL streptomycin to limit contaminations. Superficial blood vessels were carefully extracted using dissection pliers. The tissues were minced finely and enzymatically (0.25% trypsin, 37 °C, 15 min) dissociated to produce single cells. After filtered through a 100 μm pore mesh, the cell suspension was centrifuged at 800 g for 4 min and resuspended in DMEM containing 20% FBS, 100 U/mL penicillin and 100 μg/mL

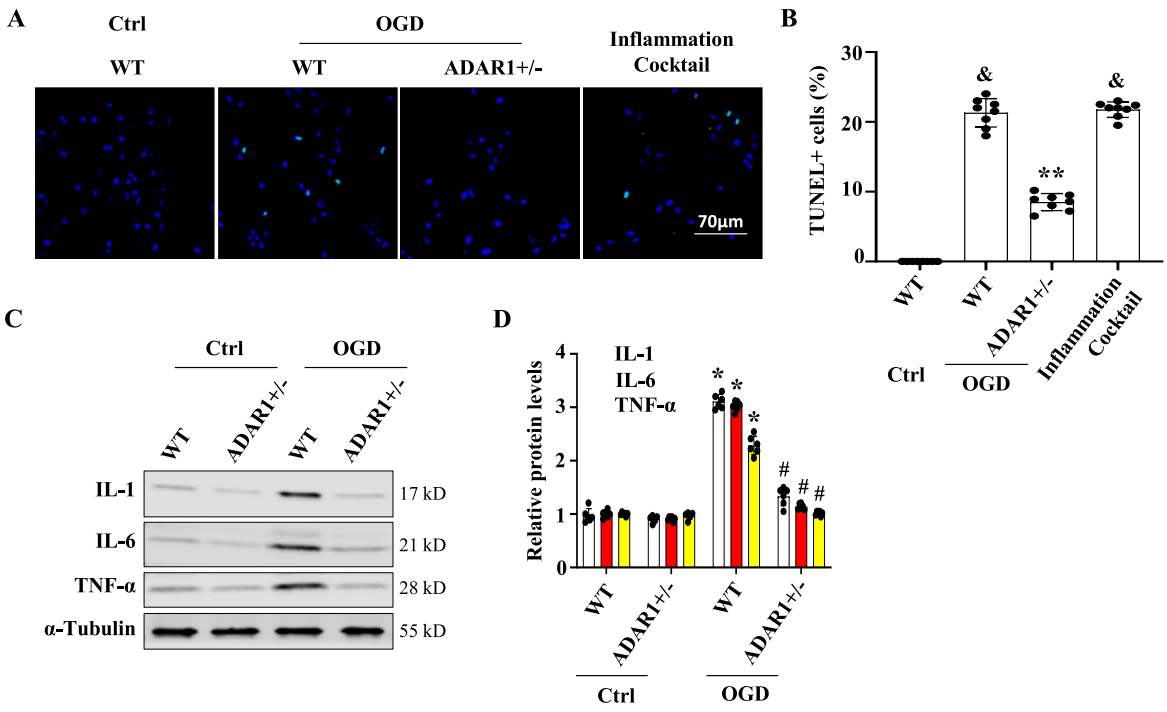

Fig. 7. Astrocyte ADAR1 promotes neuron apoptosis by secretion of pro-inflammatory cytokines IL-1, IL-6 and TNF-α. Astrocytes were primary cultured from wild type (WT) and ADAR ±mice. **(A–B)** Primary neurons were treated with astrocytes-conditioned medium with or without (Ctrl) oxygen-glucose-deprivation (OGD). Inflammation cocktail containing IL-1 (10 ng/ml), IL-6 (10 ng/ml) and TNF-α (10 ng/ml) was used as a positive control. TUNEL staining of cultured neuron (**A**), and TUNEL + cells were quantified relative to the total neuron cells (**B**). $^{\&}P < 0.01$ vs. neuron cells treated with WT astrocyte-conditioned medium without OGD (WT, Ctrl); $^{**}P < 0.01$ vs. WT astrocyte-conditioned medium with OGD (WT, OGD); n = 8. (**C-D**) Western blot analyses of IL-1, IL-6, and TNF-α production in primary astrocytes cultured with or without Oxygen-Glucose-Deprivation (OGD) for 24 h (**C**). The protein levels in C were quantified by normalizing to α-Tubulin (**D**). $^{*}P < 0.01$ vs. WT astrocytes without OGD (WT, Ctrl); $^{\#}P < 0.05$ vs. WT astrocytes with OGD (WT, OGD); n = 6.

streptomycin. The cells were plated in tissue flasks pre-coated with gelatin and matrigel at a density of 3-5 × 10^5 cells/cm^2, then cultured at 37 °C in a 95% air/5% CO2 incubator. In the medium, 10 μM forskolin (FSK) and 10 ng/mL glial cell line-derived neurotrophic factor (GDNF) were supplemented to promote cell proliferation and survival, respectively. The medium change occurred once every two days. When cells grew to confluence (10–14 d), flasks were shaken on a rotary shaker at 260 rpm for 18–20 h at 37 °C to remove the loosely attached contaminated microglia and oligodendrocyte progenitor cells (OPCs). The attached enriched astrocytes were subsequently detached using trypsin-EDTA and then subjected to different treatments.

2.16. Primary cortical neuronal cultures

Embryonic cortical neurons were isolated by standard procedures [25]. E16.5 embryonic cerebral cortices were treated with 0.25% Trypsin-EDTA and dissociated into single cells by gentle trituration. Cells were suspended in neurobasal medium supplemented with B27 and 2 mM Glut Amax, then plated on coverslips or dishes coated with poly-L-Lysine (0.05 mg/mL) diluted in boric buffer. Enrichment of neuronal culture was performed using both a previously reported method and a modified protocol [26]. Half of the medium was then replaced every 2 days until treatment.

2.17. Construction of adenoviral vector

Adenovirus expressing ADAR1 shRNA (Ad-shADAR1) was generated and purified as described previously [27]. cDNA fragment encoding the full length of human ADAR1 was amplified from ADAR1 plasmid (DNASU, HsCD00076320) by PCR, and then inserted into the pShuttle-IRES-hrGPF-1 vector (Agilent) through XhoI site. ADAR1 cDNA in the vector was verified by sequencing. Green fluorescent protein (GFP)-expressing adenovirus (Ad-GFP) was used as a control.

2.18. Triphenyltetrazolium chloride (TTC) staining

Brain tissues were quickly removed and sliced into 2 mm coronal sections using a brain matrix (Ted Pella, Redding, CA, U.S.A.). The section level was marked with bregma level. Sliced brain tissues were immersed at 37 °C for 20 min in 2% TTC (Sigma) and fixed in 10% formalin for 24 h. The images of the stained tissues were captured using a camera (Canon EOS M5). Images were analyzed using Image J (NIH, U.S.A.) in order to evaluate the infarct volume. The proportion of the ischemic area (%) was determined by the following formula: infarction area/whole section area × 100.

2.19. Statistical analysis

All experiments were repeated at least for three times. Electronic laboratory notebook was not used. All data represent independent data points but not technical replicates. Data are presented as the mean ± SD. Normality of data was assessed by the D'Agostino & Pearson normality test with alpha = 0.05. For comparisons of two groups, student's unpaired two-tailed *t*-test was used for normally distributed data, and Mann-Whitney two tailed test was used for non-normally distributed data or for groups with n less than 7. For more than 2 groups, 1-way ANOVA with Tukey post-test analysis was used for normally distributed data and Kruskal-Walli's test with Dunn's multiple comparisons test was used for non-normally distributed data. Prism 9.0 (GraphPad Software, CA) or RStudio (Desktop 1.4.1717) was used for statistical analyses, and differences considered statistically significant when nominal $P < 0.05$ or adjusted $P < 0.05$ in case of multiple testing.

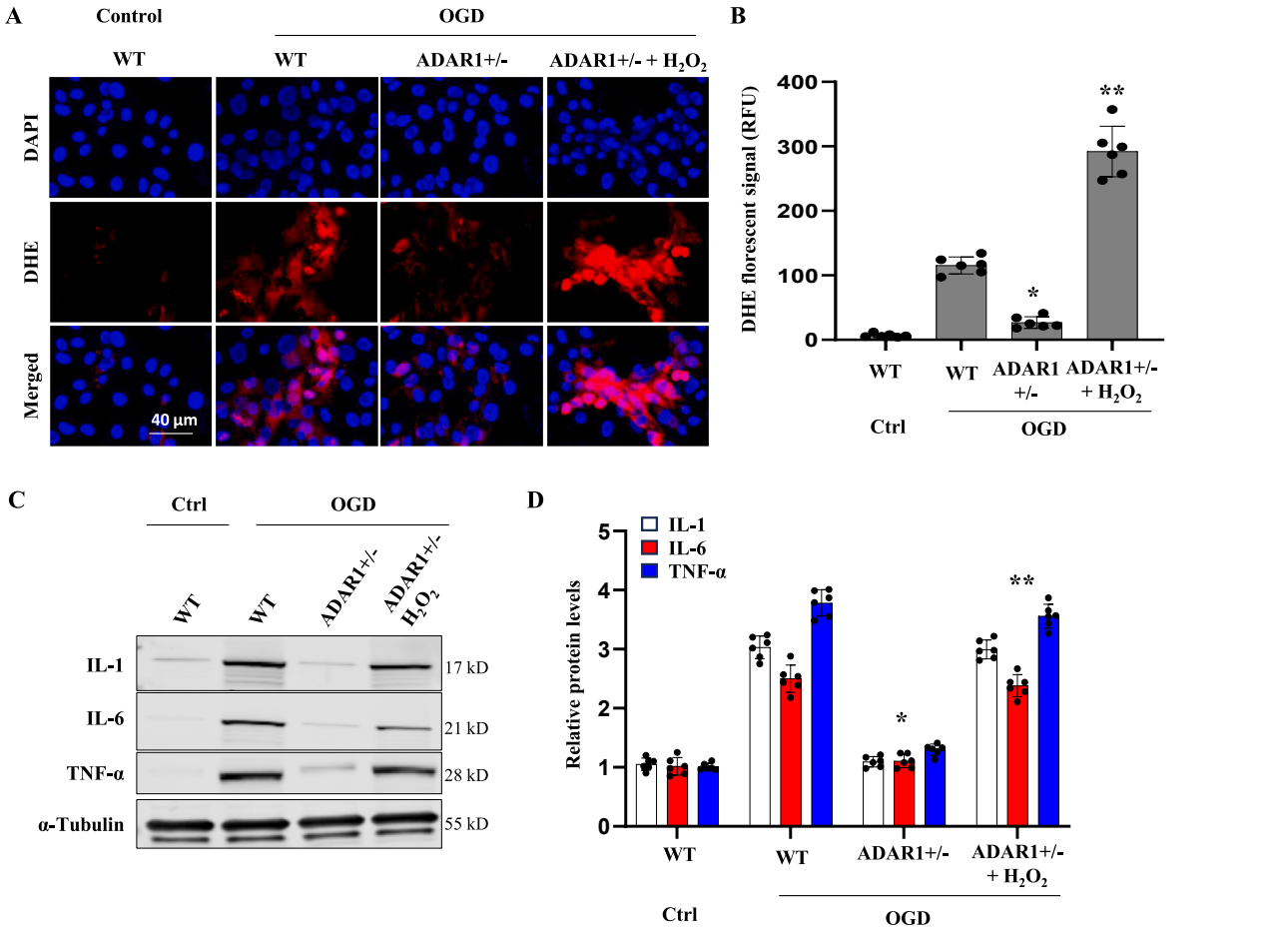

Fig. 8. ADAR1 promotes the production of pro-Inflammatory cytokines via ROS in astrocytes. Astrocytes were primary cultured from wild type (WT) and ADAR ±mice. **A,** Representative DHE fluorescent images showing the ROS levels. **B**, ROS levels in A were quantified relative to the WT control (Ctrl) group. **C-D**, Western blot analyses of IL-1, IL-6 and TNF-α production in primary astrocytes cultured with or without Oxygen-Glucose-Deprivation (OGD) and H_2O_2 (0.1 mM) for 24 h **(C)**. The protein levels were quantified by normalizing to α-Tubulin (**D**). *P < 0.05 vs. WT astrocytes with OGD (WT, OGD); **P < 0.05 vs. ADAR1 ± astrocytes with OGD (ADAR1+/−, OGD); n = 6.

3. Results

3.1. ADAR1 is highly induced in astrocytes in ischemic brain of MCAO-operated mice

To investigate the potential involvement of ADAR1 in the pathogenesis of ischemic stroke, we employed a widely used experimental model of ischemic stroke induced by MCAO. ADAR1 is not normally expressed in astrocytes. However, immunofluorescent co-staining of ADAR1 with glial fibrillary acidic protein (GFAP) in the glial scar and ischemic area of mice with MCAO revealed a significant induction of ADAR1 expression in astrocytes in the ischemic brain (Fig. 1A). The quantification of the GFAP + ADAR1+ cells showed that more than 35% of astrocytes expressed ADAR1 in response to ischemic injury (Fig. 1B). Time course examination of ADAR1 expression showed that ADAR1 was highly induced as early as one day after the MCAO, and the high level of expression was maintained for 7–14 days although the protein level was declined at 14 days (Fig. 1C–E), possibly through post-translational mechanisms such as degradation because the mRNA levels are still high at this time (Fig. 1C). It appeared that both p150 and p110 isoforms were significantly upregulated. These findings suggest that ADAR1 may play a role in the astrocytic response to ischemic stroke.

3.2. ADAR1 deficiency reduces brain infarct areas and improves neurobehavioral outcomes

To determine if ADAR1 is essential for ischemic stroke development, we generated the MCAO stroke model in wild type (WT) and (ADAR1+/−) mice. ADAR ±mice were used because ADAR1−/− mice is embryonically lethal. ADAR1 ± mice showed a significant decrease in infarct volume compared to wild-type (WT) mice (Fig. 2A and B), suggesting that ADAR1 plays a critical role in the stroke development. In addition to the reduction in infarct volume, ADAR1 ± mice exhibited improved neurobehavioral outcomes compared to WT mice. Specifically, in the rotarod test, ADAR1 ± mice had a significantly increased latency to fall, indicating improved motor coordination and balance (Fig. 2C). Similarly, in the elevated body swing test, ADAR1 ± mice spent less time bending towards the right side, indicating improved postural balance and motor coordination (Fig. 2D). In the corner test, ADAR1 ± mice made fewer ipsilateral turns, suggesting improved sensorimotor integration and coordination (Fig. 2E). Finally, ADAR1 ± mice also exhibited greater grip strength compared to WT mice, further supporting their improved motor function (Fig. 2F). These findings indicated that ADAR1 deficiency not only reduces the extent of ischemic brain injury, but also results in improved recovery of motor function following stroke.

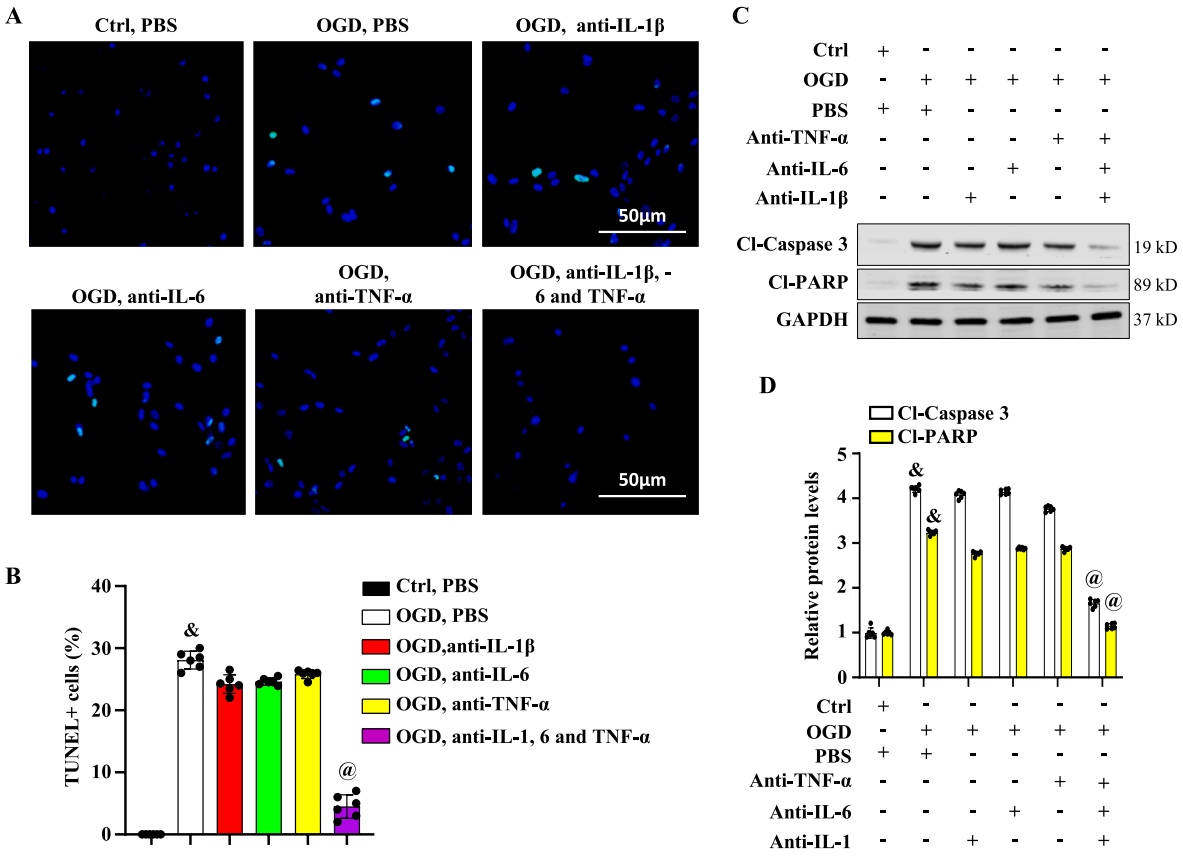

Fig. 9. Neutralizing antibody cocktail against IL-1, 6 and TNF-α blocks neuron cell apoptosis caused by activated astrocytes. Primary neurons were treated with astrocyte-conditioned medium with or without (Ctrl) oxygen-glucose-deprivation (OGD). The medium was supplemented with PBS or neutralizing antibodies against IL-1β, −6 and/or TNF-α, as indicated. (**A-B**) TUNEL staining of neuron cells treated with astrocyte-conditioned medium (**A**), and TUNEL + cells were quantified relative to the total neuron cells (**B**). $^{\&}P < 0.01$ vs. group without OGD (Ctrl, PBS); $^{@}P < 0.01$ vs. group with OGD & PBS (OGD, PBS); n = 6. (**C-D**) Cleaved-Caspase 3 and Cleaved-PARP levels were detected by Western blot (**C**) and quantified by normalizing to GAPDH (**D**). $^{\&}P < 0.01$ vs. group without OGD (Ctrl, PBS); $^{@}P < 0.01$ vs. group with OGD & PBS (OGD, PBS) for the corresponding proteins, respectively; n = 6.

3.3. ADAR1 deficiency inhibits glial cell activation in mouse brain with MCAO

The activation of astrocytes and microglia is crucial for the pathogenesis of ischemic stroke and also plays a pivotal role in the recovery process. To determine whether ADAR1 deficiency affects glial cell activation in the ischemic brain, we immuno-stained astrocyte marker GFAP and microglia/macrophage-specific calcium-binding protein Iba-1 in the ischemic areas of mouse brains (Fig. 3A and B). The results showed that ADAR1 deficiency significantly reduced the expression of both GFAP and Iba-1 in the ischemic areas of the mouse brains (Fig. 3C and D). These findings were further confirmed by Western blot analyses, which showed that ADAR1 deficiency resulted in decreased levels of GFAP, Iba-1, and CD11b in the ischemic brain (Fig. 3, E-F). The data suggest that ADAR1 deficiency inhibits astrocyte and microglia activation in the ischemic brain, which may contribute to the observed reductions in brain infarct area and improved neurobehavioral outcomes. Astrocytes and microglia play critical roles in regulating the inflammatory response and neurotoxicity following stroke, and the activation of astrocytes and microglia is a hallmark of the inflammatory response to ischemic injury, leading to release of pro-inflammatory cytokines or chemokines, which exacerbate brain injury. Inhibition of astrocyte and microglia activation has been shown to reduce brain injury and improve functional recovery in ischemic stroke models. Therefore, our findings suggest that ADAR1 may promote ischemic stroke by regulating glial cell activation and reducing inflammation in the ischemic brain.

3.4. ADAR1 deficiency inhibits astrocyte proliferation and migration

Co-immunostaining of Ki-67 with GFAP in glial scar revealed reduced proliferation in ADAR1-deficient mice (Fig. 4A). To elucidate the underlying mechanism by which ADAR1 regulates astrocyte proliferation, we detected the potential activation of ERK and PI3K/Akt signaling pathways because they are involved in regulating astrocyte proliferation. Western blot analyses of WT and ADAR1 ± mouse ischemic brain tissues showed that along with the downregulation of cell proliferation markers PCNA and Ki-67, ADAR ±significantly inhibited ERK and Akt phosphorylation that was induced in WT mouse brain by MCAO (Fig. 4B and C). To determine if ERK and Akt signaling is important for ADAR1-meidated astrocyte proliferation, primary astrocytes were overexpressed with ADAR1 and treated with PI3/Akt (LY294002) or MEK/ERK (U0126) inhibitor. As shown in Fig. 4D and E, blocking Akt signaling, but not the ERK pathway, blocked ADAR1-promoted PCNA and Ki67 expression. These results suggested that ADAR1 mediates astrocyte proliferation by promoting the Akt signaling pathway. We further confirmed the role of ADAR1 in astrocyte proliferation by immunostaining of Ki-67 in primary astrocytes isolated from WT and ADAR ±mice (Fig. 5A).

Since astrocyte migration is also important for stroke, we investigated the effect of ADAR1 on the migration of astrocytes by wound healing assay. Confluent monolayers of primary cultured wild-type or ADAR1 ± astrocytes were scratched, and the recovery of wounded areas was observed using an inverted phase-contrast microscope. As shown in Fig. 5B, ADAR1 deficiency inhibited astrocyte migration. *Trans*-well assays further confirmed that ADAR1 is essential for astrocyte migration

(Fig. 5C).

3.5. ADAR1 deficiency inhibits activated astrocyte-caused neuron apoptosis in stroke brain

Although mechanisms underlying neuron death following brain ischemic stroke are not fully understood, cell apoptosis is known to be a significant contributor. TUNEL staining showed that MCAO caused significant cell death following the stroke. However, ADAR1 ± blocked the MCAO-induced apoptosis (Fig. 6A and B). Consistently, ADAR1 ± blocked the cleaved-Caspase 3 and cleaved-PARP levels that were significantly increased in mouse brains with MCAO, demonstrating that ADAR1 contributes to the neuron death in the stroke brain (Fig. 6C and D). Moreover, ADAR1 ± decreased the expression of pro-inflammatory cytokines IL-1β, IL-6 and TNF-α, which was increased by MCAO in the WT mice (Fig. 6, E-F), suggesting a potential link between ADAR1 and inflammatory responses in brain ischemia. These results are consistent with previous studies showing the involvement of ADAR1 in modulating inflammation and apoptosis in various cellular contexts [28–34].

3.6. Astrocyte ADAR1 induces neuron apoptosis by secreting IL-1β, IL-6 and TNF-α

In ischemic stroke, pro-inflammatory cytokines produced by astrocytes and microglia, including IL-1, IL-6, and TNF-α, have been shown to play a crucial role in the pathogenesis of brain damage. To determine if ADAR1 regulates neuron apoptosis through astrocyte-mediated inflammation, we cultured the primary astrocytes in the Oxygen-Glucose-Deprivation (OGD) condition for 24 h, and used the astrocyte-conditioned medium to treat neuron cells. TUNEL staining of astrocyte-conditioned medium-treated neuron showed a significant increase in apoptosis (Fig. 7A and B). However, ADAR ±blocked the apoptosis (Fig. 7A and B). Importantly, the inflammation cocktail containing IL-1β, IL-6, and TNF-α also induced neuron apoptosis (Fig. 7A). Western blot analyses showed the induction of IL-1β, IL-6, and TNF-α in primary wild type astrocytes, but it was blocked in ADAR1 ± astrocytes (Fig. 7, B–C). These results suggest that ADAR1 in astrocytes promotes neuron apoptosis by producing pro-inflammatory cytokines.

Oxidative stress, characterized by an imbalance between the production and removal of reactive oxygen species (ROS), is a pivotal factor in the pathogenesis of ischemic stroke. During ischemia, the overproduction of ROS can cause cellular damage, leading to neuronal death and exacerbation of inflammation [9,10]. The impact of ROS on ischemic stroke extends to the activation of glial cells, disruption of the blood-brain barrier, and modulation of signaling pathways that influence cell survival and apoptosis. We hypothesized that ADAR1 plays a role connecting oxidative stress to the inflammatory response in astrocytes. Indeed, OGD increased ROS levels in WT astrocytes, as indicated by DHE staining (Fig. 8A and B), which correlated with elevated cytokines (Fig. 8C and D). However, ADAR1+−/− decreased the ROS along with cytokine production (Fig. 8). To determine if ADAR1 controls cytokine release via ROS, we treated ADAR1 ± cells with H_2O_2 to restore the ROS (Fig. 8A and B) and found that H_2O_2 treatment abolished the effect of ADAR1 deficiency in reducing cytokine secretion (Fig. 8, C-D). These results provided strong evidence to support the interplay between ADAR1 and oxidase stress in controlling cytokine release.

3.7. Neutralizing antibody cocktail against IL-1β, IL-6 and TNF-α prevented neuron from apoptosis

To explore the potential association between ADAR1-mediated release of pro-inflammatory cytokines IL-1β, IL-6, and TNF-α in astrocytes and the neuron apoptosis, neutralizing antibodies against IL-1β, IL-6, and TNF-α were added individually or in combination to astrocyte culture medium. Then, the neuron cells were treated with the astrocyte-conditioned medium. TUNEL staining of neurons treated with astrocyte-conditioned medium containing all three antibodies, but not the individual antibody, showed a decrease in apoptosis (Fig. 9A and B). Western blotting showed a dramatic decrease in cleaved-Caspase 3 and cleaved-PARP levels in neurons treated with the cocktail of neutralizing antibodies-containing astrocyte-conditioned medium, but not with the individual antibodies (Fig. 9, C-D). These findings indicated that IL-1β, IL-6, and TNF-α are all required for the neuron apoptosis induced by astrocytes, and thus blocking all three cytokines with neutralizing antibody cocktail may be a potential effective therapeutic approach to prevent neuron death following brain ischemic stroke.

4. Discussions

Ischemic stroke is the most common type of stroke, causing neuronal loss and gliosis and inflammation in the surrounding ischemic core [35,36]. Our study using the MCAO mouse model reveals that ADAR1 plays a critical role in stroke progression. ADAR1 is induced in the mouse ischemic brain area. ADAR1 ± significantly reduces the infarct volume after MCAO, resulting in better neurobehavioral outcomes. Furthermore, ADAR1 deficiency reduces the number of microglia and activated astrocytes in the ischemic brain area, indicating that ADAR1 promotes stroke progression by mediating astrocyte and microglia proliferation. Our study suggests that the response of microglia is secondary to that of astrocytes in mediating ADAR1 function, as the up-regulation of ADAR1 occurs mainly in astrocytes.

Astrocytes play a pivotal role in the pathophysiology of ischemic stroke. Their activation has both beneficial and detrimental effects. Our studies reveal that ADAR1 promotes astrocyte proliferation and possibly migration via the Akt signaling pathway while suppressing neuron apoptosis in the mouse brains with MCAO treatment. Additionally, ADAR1 promotes the production and secretion of pro-inflammatory cytokines IL-1β, IL-6, and TNF-α in astrocytes, which causes neuron apoptosis. Most importantly, neutralizing antibodies against these cytokines diminish the astrocyte ADAR1-mediated neuron apoptosis. Consistent with our observations, elevation of IL-1β, IL-6, and TNF-α levels is found in human brain and blood after ischemic stroke [37]. Moreover, therapies targeting IL-1β, IL-6, and TNF-α have been developed and used in various inflammatory and autoimmune diseases [38–40]. Our study shows that targeting only one cytokine may not be effective for stroke therapy as these cytokines often act synergistically [41]. Therefore, a cocktail of neutralizing antibodies against IL-1β, IL-6, and TNF-α is used to prevent neuron apoptosis in our study. Surprisingly, individual blockade of each of IL-1β, IL-6, or TNF-α cannot prevent neuron death caused by activated astrocytes. However, dramatic inhibition of the apoptosis is achieved by using a combination of neutralizing antibodies against all three cytokines. Therefore, our study provides a rationale for using neutralizing antibody cocktail as a potentially effective approach to treat ischemic stroke.

Our findings further elucidate the mechanistic relationship between ADAR1 and the secretion of pro-inflammatory cytokines through the modulation of oxidative stress. The primary cultured astrocytes from WT and ADAR ±mice exhibit differential responses to OGD. ADAR1 ± cells exhibit decreased ROS and cytokine production. The interplay between ADAR1 and oxidase stress provides critical insights into how ADAR1 enhances the secretion of cytokines like IL-1, IL-6, and TNF-α, which may open additional new avenues for therapeutic interventions to reduce infarct volume and improve neurobehavioral outcomes.

Funding information

This work was supported by grants from National Institutes of Health (HL117247, HL119053, and HL147313), Department of Veterans Affairs Merit Review Awards (I01 BX006161), and the University of Missouri School of Medicine TRIUMPH Initiative Funding. DC is a recipient of American Heart Association Postdoctoral Fellowship award (#657293).

Declaration of competing interest

Authors declare that there are no conflicts of interest.

Data availability

Data will be made available on request.

Acknowledgments

None.

References

[1] E.S. Donkor, Stroke in the 21(st) century: a snapshot of the burden, epidemiology, and quality of life, Stroke Res. Treat. 2018 (2018), 3238165, https://doi.org/10.1155/2018/3238165.

[2] S.S. Virani, A. Alonso, E.J. Benjamin, M.S. Bittencourt, C.W. Callaway, A.P. Carson, A.M. Chamberlain, A.R. Chang, S. Cheng, F.N. Delling, et al., Heart disease and stroke statistics-2020 update: a report from the American Heart association, Circulation 141 (2020) e139–e596, https://doi.org/10.1161/CIR.0000000000000757.

[3] C. Xing, K. Arai, E.H. Lo, M. Hommel, Pathophysiologic cascades in ischemic stroke, Int. J. Stroke 7 (2012) 378–385, https://doi.org/10.1111/j.1747-4949.2012.00839.x.

[4] R.L. Jayaraj, S. Azimullah, R. Beiram, F.Y. Jalal, G.A. Rosenberg, Neuroinflammation: friend and foe for ischemic stroke, J. Neuroinflammation 16 (2019) 142, https://doi.org/10.1186/s12974-019-1516-2.

[5] H. Xu, E. Wang, F. Chen, J. Xiao, M. Wang, Neuroprotective phytochemicals in experimental ischemic stroke: mechanisms and potential clinical applications, Oxid. Med. Cell. Longev. 2021 (2021), 6687386, https://doi.org/10.1155/2021/6687386.

[6] V. Banwell, E.S. Sena, M.R. Macleod, Systematic review and stratified meta-analysis of the efficacy of interleukin-1 receptor antagonist in animal models of stroke, J. Stroke Cerebrovasc. Dis. 18 (2009) 269–276, https://doi.org/10.1016/j.jstrokecerebrovasdis.2008.11.009.

[7] A. Moretti, F. Ferrari, R.F. Villa, Neuroprotection for ischaemic stroke: current status and challenges, Pharmacol. Ther. 146 (2015) 23–34, https://doi.org/10.1016/j.pharmthera.2014.09.003.

[8] S.K. McCann, F. Cramond, M.R. Macleod, E.S. Sena, Systematic review and meta-analysis of the efficacy of interleukin-1 receptor antagonist in animal models of stroke: an update, Transl Stroke Res 7 (2016) 395–406, https://doi.org/10.1007/s12975-016-0489-z.

[9] Y. Li, Y. Wang, W. Yang, Z. Wu, D. Ma, J. Sun, H. Tao, Q. Ye, J. Liu, Z. Ma, et al., ROS-responsive exogenous functional mitochondria can rescue neural cells post-ischemic stroke, Front. Cell Dev. Biol. 11 (2023), 1207748, https://doi.org/10.3389/fcell.2023.1207748.

[10] H. Ye, Z. Ma, L. Liu, T. Zhang, Q. Han, Z. Xiang, Y. Xia, Y. Ke, X. Guan, Q. Shi, et al., Thrombus inhibition and neuroprotection for ischemic stroke treatment through platelet regulation and ROS scavenging, ChemMedChem 17 (2022), e202200317, https://doi.org/10.1002/cmdc.202200317.

[11] N. Mannion, F. Arieti, A. Gallo, L.P. Keegan, M.A. O'Connell, New insights into the biological role of mammalian ADARs; the RNA editing proteins, Biomolecules 5 (2015) 2338–2362, https://doi.org/10.3390/biom5042338.

[12] E. Eisenberg, E.Y. Levanon, A-to-I RNA editing - immune protector and transcriptome diversifier, Nat. Rev. Genet. 19 (2018) 473–490, https://doi.org/10.1038/s41576-018-0006-1.

[13] J.H. Yang, X. Luo, Y. Nie, Y. Su, Q. Zhao, K. Kabir, D. Zhang, R. Rabinovici, Widespread inosine-containing mRNA in lymphocytes regulated by ADAR1 in response to inflammation, Immunology 109 (2003) 15–23, https://doi.org/10.1046/j.1365-2567.2003.01598.x.

[14] G. Wang, H. Wang, S. Singh, P. Zhou, S. Yang, Y. Wang, Z. Zhu, J. Zhang, A. Chen, T. Billiar, et al., ADAR1 prevents liver injury from inflammation and suppresses interferon production in hepatocytes, Am. J. Pathol. 185 (2015) 3224–3237, https://doi.org/10.1016/j.ajpath.2015.08.002.

[15] Z. Shangxun, L. Junjie, Z. Wei, W. Yutong, J. Wenyuan, L. Shanshou, W. Yanjun, W. Qianmei, F. Zhusheng, Y. Chaoping, et al., ADAR1 alleviates inflammation in a murine sepsis model via the ADAR1-miR-30a-SOCS3 Axis, Mediat. Inflamm. 2020 (2020), 9607535, https://doi.org/10.1155/2020/9607535.

[16] V.H. Brait, K.A. Jackman, T.Y. Pang, Effects of wheel-running on anxiety and depression-relevant behaviours in the MCAO mouse model of stroke: moderation of brain-derived neurotrophic factor and serotonin receptor gene expression, Behav. Brain Res. 432 (2022), 113983, https://doi.org/10.1016/j.bbr.2022.113983.

[17] L. Li, L. Dong, Z. Xiao, W. He, J. Zhao, H. Pan, B. Chu, J. Cheng, H. Wang, Integrated analysis of the proteome and transcriptome in a MCAO mouse model revealed the molecular landscape during stroke progression, J. Adv. Res. 24 (2020) 13–27, https://doi.org/10.1016/j.jare.2020.01.005.

[18] F.F. Alamri, A.A. Shoyaib, A. Biggers, S. Jayaraman, J. Guindon, V.T. Karamyan, Applicability of the grip strength and automated von Frey tactile sensitivity tests in the mouse photothrombotic model of stroke, Behav. Brain Res. 336 (2018) 250–255, https://doi.org/10.1016/j.bbr.2017.09.008.

[19] M. Balkaya, J.M. Krober, A. Rex, M. Endres, Assessing post-stroke behavior in mouse models of focal ischemia, J. Cerebr. Blood Flow Metabol. 33 (2013) 330–338, https://doi.org/10.1038/jcbfm.2012.185.

[20] E. Ingberg, J. Gudjonsdottir, E. Theodorsson, A. Theodorsson, J.O. Strom, Elevated body swing test after focal cerebral ischemia in rodents: methodological considerations, BMC Neurosci. 16 (2015) 50, https://doi.org/10.1186/s12868-015-0189-8.

[21] J.D. Christensen, The rotacone: a new apparatus for measuring motor coordination in mice, Acta Pharmacol. Toxicol. 33 (1973) 255–261, https://doi.org/10.1111/j.1600-0773.1973.tb01525.x.

[22] R.M. Deacon, Measuring motor coordination in mice, J. Vis. Exp. (2013), e2609, https://doi.org/10.3791/2609.

[23] R-j Liao, J. Lei, R-r Wang, H-w Zhao, Y. Chen, Y. Li, L. Wang, L.-Y. Jie, y-D Zhou, X. Zhang, et al., Histidine provides long-term neuroprotection after cerebral ischemia through promoting astrocyte migration, Sci. Rep. 5 (2015), 15356, https://doi.org/10.1038/srep15356.

[24] R. Ran, D. Cai, S.D. King, X. Que, J.M. Bath, S.Y. Chen, Surfactant protein A, a novel regulator for smooth muscle phenotypic modulation and vascular remodeling-brief report, Arterioscler. Thromb. Vasc. Biol. 41 (2021) 808–814, https://doi.org/10.1161/ATVBAHA.120.314622.

[25] L.G. Hilgenberg, M.A. Smith, Preparation of dissociated mouse cortical neuron cultures, J. Vis. Exp. (2007) 562, https://doi.org/10.3791/562.

[26] M.P. Sahu, O. Nikkila, S. Lagas, S. Kolehmainen, E. Castren, Culturing primary neurons from rat hippocampus and cortex, Neuronal Signal 3 (2019), NS20180207, https://doi.org/10.1042/NS20180207.

[27] D. Cai, C. Sun, G. Zhang, X. Que, K. Fujise, N.L. Weintraub, S.Y. Chen, A novel mechanism underlying inflammatory smooth muscle phenotype in abdominal aortic aneurysm, Circ. Res. 129 (2021) e202–e214, https://doi.org/10.1161/CIRCRESAHA.121.319374.

[28] Y. Jiang, Z. Wang, X. Chen, W. Wang, X. Wang, ADAR1 silencing-induced HUVEC apoptosis is mediated by FGFR2 under hypoxia stress, Drug Des. Dev. Ther. 12 (2018) 4181–4189, https://doi.org/10.2147/DDDT.S181312.

[29] M. Sakurai, Y. Shiromoto, H. Ota, C. Song, A.V. Kossenkov, J. Wickramasinghe, L. C. Showe, E. Skordalakes, H.Y. Tang, D.W. Speicher, et al., ADAR1 controls apoptosis of stressed cells by inhibiting Staufen1-mediated mRNA decay, Nat. Struct. Mol. Biol. 24 (2017) 534–543, https://doi.org/10.1038/nsmb.3403.

[30] A.M. Toth, Z. Li, R. Cattaneo, C.E. Samuel, RNA-specific adenosine deaminase ADAR1 suppresses measles virus-induced apoptosis and activation of protein kinase PKR, J. Biol. Chem. 284 (2009) 29350–29356, https://doi.org/10.1074/jbc.M109.045146.

[31] O.A. Vogel, J. Han, C.Y. Liang, S. Manicassamy, J.T. Perez, B. Manicassamy, The p150 isoform of ADAR1 blocks sustained RLR signaling and apoptosis during influenza virus infection, PLoS Pathog. 16 (2020), e1008842, https://doi.org/10.1371/journal.ppat.1008842.

[32] C.R. Walkley, B.T. Kile, Cell death following the loss of ADAR1 mediated A-to-I RNA editing is not effected by the intrinsic apoptosis pathway, Cell Death Dis. 10 (2019) 913, https://doi.org/10.1038/s41419-019-2160-6.

[33] Q. Wang, M. Miyakoda, W. Yang, J. Khillan, D.L. Stachura, M.J. Weiss, K. Nishikura, Stress-induced apoptosis associated with null mutation of ADAR1 RNA editing deaminase gene, J. Biol. Chem. 279 (2004) 4952–4961, https://doi.org/10.1074/jbc.M310162200.

[34] C.C. Yang, Y.T. Chen, Y.F. Chang, H. Liu, Y.P. Kuo, C.T. Shih, W.C. Liao, H. W. Chen, W.S. Tsai, B.C. Tan, ADAR1-mediated 3' UTR editing and expression control of antiapoptosis genes fine-tunes cellular apoptosis response, Cell Death Dis. 8 (2017), e2833, https://doi.org/10.1038/cddis.2017.12.

[35] I.K. Koutsaliaris, I.C. Moschonas, L.M. Pechlivani, A.N. Tsouka, A.D. Tselepis, Inflammation, oxidative stress, vascular aging and atherosclerotic ischemic stroke, Curr. Med. Chem. (2021), https://doi.org/10.2174/0929867328666210921161711.

[36] M.A. Jacob, M.S. Ekker, Y. Allach, M. Cai, K. Aarnio, A. Arauz, M. Arnold, H.J. Bae, L. Bandeo, M.A. Barboza, et al., Global differences in risk factors, etiology, and outcome of ischemic stroke in young adults-A worldwide meta-analysis: the GOAL initiative, Neurology 98 (2022) e573–e588, https://doi.org/10.1212/WNL.0000000000013195.

[37] B.H. Clausen, M. Wirenfeldt, S.S. Hogedal, L.H. Frich, H.H. Nielsen, H.D. Schroder, K. Ostergaard, B. Finsen, B.W. Kristensen, K.L. Lambertsen, Characterization of the TNF and IL-1 systems in human brain and blood after ischemic stroke, Acta Neuropathol Commun 8 (2020) 81, https://doi.org/10.1186/s40478-020-00957-y.

[38] S. Yusuf, Y. Soenarto, M. Juffrie, W. Lestariana, The effect of zinc supplementation on pro-inflammatory cytokines (TNF-alpha, IL-1 AND IL-6) in mice with Escherichia coli LPS-induced diarrhea, Iran. J. Microbiol. 11 (2019) 412–418.

[39] Y. Chen, W. Huang, Z. Li, Y. Duan, Z. Liang, H. Zhou, C. Tang, The effect of acupuncture on the expression of inflammatory factors TNF-alpha, IL-6,IL-1 and CRP in cerebral infarction: a protocol of systematic review and meta-analysis, Medicine (Baltim.) 98 (2019), e15408, https://doi.org/10.1097/MD.0000000000015408.

[40] P.W. Yuan, D.Y. Liu, X.D. Chu, Y.Q. Hao, C. Zhu, Q. Qu, Effects of preventive administration of juanbi capsules on TNF-alpha, IL-1 and IL-6 contents of joint fluid in the rabbit with knee osteoarthritis, J. Tradit. Chin. Med. 30 (2010) 254–258, https://doi.org/10.1016/s0254-6272(10)60052-0.

[41] B.H. Clausen, K.L. Lambertsen, F. Dagnaes-Hansen, A.A. Babcock, C.U. von Linstow, M. Meldgaard, B.W. Kristensen, T. Deierborg, B. Finsen, Cell therapy centered on IL-1Ra is neuroprotective in experimental stroke, Acta Neuropathol. 131 (2016) 775–791, https://doi.org/10.1007/s00401-016-1541-5.